Supplementary Information

A Smart Photodynamic Ionic Liquid Nanogel Fiber-Based Actuator with Efficient Photothermal Conversion and Self-Cleaning Based on Supramolecular Assembly

Meng Ju, Mengting Wu, Keting Li, Aiqin Hou, Kongliang Xie*,Mengyuan Yue, Aiqin Gao*

Methods

Materials. 4-nitrophthalonitrile, p-hydroxybenzoic acid and 1,8-diazabicyclo [5.4.0] undec-7-ene (DBU) and 1, 3-diphenylisobenzofuran (DPBF) were purchased from Adamas Reagent Co., Ltd., Shanghai, China. Other chemicals used in the synthesis were purchased from Sinopharm Chemical Reagent Co., Ltd., Shanghai, China and used without the further purification.

Synthesis of the Azobenzene-Imidazole Ionic Liquid and the Designed Ionic Liquid Disk-Like Molecules (AzoPc1).

The detailed synthesis routes for Azo1 and AzoPc1, also FT-IR, ^{1}HNMR, ^{13}CNMR, ^{19}F NMR and MS of the target compounds are shown in Fig. S1- Fig. S17.

Synthesis of Azo1

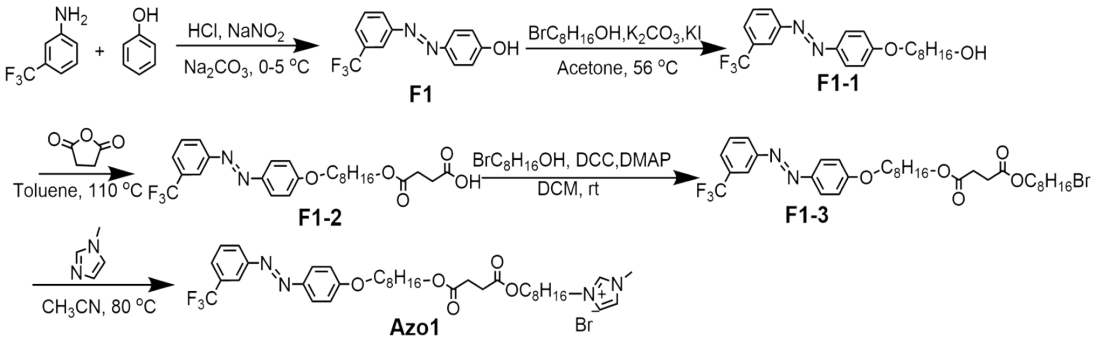

Fig. S1 Synthetic route of Azo1.

7.5 mL of hydrochloric acid at a concentration of 36% was added to 50 mL of water for diluting. 3-Trifluoromethylaniline (5.00 g, 0.03 mol) was weighed and dissolved in the above aqueous hydrochloric acid solution, stirred and cooled down in an ice bath to 0-5 °C. $NaNO_2$ (2.07 g, 0.03 mol) was then weighed and prepared as an aqueous solution with a mass fraction of 30% and cooled down to 0-5°C. Finally, the aqueous $NaNO_2$ solution was slowly dripped into the 3-trifluoromethylaniline hydrochloric acid

aqueous solution and the reaction lasted for 30 min. At the end of the reaction, the excess nitrite was neutralized with sulfamic acid, and the precipitate was removed by the filtration to obtain a solution of 3-trifluoromethylaniline diazo. The coupling component was prepared by weighing out phenol (2.82 g, 0.03 mol), Na_2CO_3 (3.18 g, 0.03 mol), and $NaHCO_3$ (2.52 g, 0.03 mol), and dissolving them in 100 mL of water. After stirring, the solution was cooled to 0-5°C in an ice bath and maintained at this temperature. Subsequently, the diazo solution was slowly added to the coupling component. After the reaction lasted 30 min, the pH value was adjusted to 5-7, and the filtration was performed. Next, 40 mL of hexane was added to wash the filter cake, and the filtration was repeated to obtain F1 (7.28 g, yield 88.12%, m.p. 114-116 ^oC).

F1 (6.00 g, 22.51 mmol) was dissolved in 60 mL of acetone. Then, bromooctanol (9.42 g, 45.02 mmol), K_2CO_3 (3.11 g, 22.51 mmol) and a trace amount of KI were added and the reaction temperature was raised to 56 °C. The reaction lasted for 15 h, followed by the filtration, collection of the filtrate and removal of acetone by the rotary evaporation to give an oily crude product. Next, 50 mL of n-hexane was added to the crude product and a large amount of yellow powder was precipitated and filtrated to obtain F1-1 (7.51 g, yield 84.48%, m.p. 76-78 ^oC).

F1-1 (7.51 g, 19.12 mmol) was dissolved in 70 mL of toluene and succinic anhydride (2.10 g, 21.03 mmol) was added and heated to 110 °C for 11 h. After the reaction, the rotary evaporation was carried out to eliminate the toluene, resulting in a red oily crude product. The product was refluxed in a methanol-water mixture (10:1 v/v), then cool and filter to obtain F1-2 (6.77 g, yield 71.90%, m.p. 79-80 °C).

F1-2 (6.77 g, 13.71 mmol) was dissolved in 20 mL of dichloromethane. Subsequently, a minor quantity of DMAP was introduced following the addition of DCC (2.82 g, 13.71 mmol) and 8-bromooctanol (2.86 g, 13.71 mmol). The reaction finished after stirring at the ambient temperature for 1 h. The insoluble substance was eliminated via the filtration and the dichloromethane was then evaporated through the centrifugation, yielding a brownish-red oily substance. The crude product was recrystallized using methanol and hexane to give the yellow powder F1-3 (7.50 g, yield 79.90%, m.p. 25-27 ^oC).

F1-3 (7.00 g, 10.22 mmol) and 20 mL of acetonitrile were introduced into the flask and agitated. N-methylimidazole (0.84 g, 10.22 mmol) was added dropwise, and the reaction system was heated to 80 °C, completing in 18 h. The solvent was eliminated using the centrifugation and evaporation, yielding a yellow crude product, which was subsequently recrystallized using 30 mL of ethyl acetate and filtrate to obtain the yellow powder Azo1 (5.30 g, yield 75.36%, m.p. 54-57 °C). FT-IR ν (cm-1): 3450 (-C=O), 3064 (-CH), 2936 (-CH), 2860 (-CH), 1720 (-C=O), 1602 (-N=N), 1502 (benzene), 1320 (C-N), 1245 (benzene), 1163 (imidazole ring), 1115 (C-C), 1019 (=C-O-C); ^{1}H NMR (400 MHz, $CDCl_3$), δ (ppm): 10.44 (s, 1H, Ar-H), 8.14-8.13 (s, 1H, Ar-H), 8.07-8.05 (dt, 1H, Ar-H), 7.95-7.93 (d, 2H, Ar-H), 7.69-7.68 (d, 1H, Ar-H), 7.64-7.62 (t, 1H, -CH=), 7.43 (d, 1H, Ar-H), 7.34-7.33 (d, 1H, Ar-H), 7.04-7.00 (m, 2H, -CH=), 4.34-4.31 (t, 2H, $-CH_2-$), 4.13 (s, 3H, $-CH_3$), 4.10-4.05 (m, 6H, $-CH_2-$), 2.63 (s, 4H, $-CH_2-$), 1.97-1.91 (m, 4H, $-CH_2-$), 1.85-1.81 (dd, 2H, $-CH_2-$), 1.50-1.47 (m, 2H, $-CH_2-$), 1.38-1.31 (m, 16H, $-CH_2-$). ^{13}C NMR (151 MHz, CDCl3), δ (ppm): 172.47, 172.44, 162.27, 152.73, 146.56, 142.35, 137.85, 129.63, 126.50, 126.47, 126.01, 125.13, 123.32, 123.04, 121.69, 119.19, 119.16, 114.81, 68.37, 64.85, 64.71, 50.16, 36.82, 30.23, 29.69, 29.22, 29.17, 29.14, 29.12, 28.87, 28.78, 28.55, 28.46, 26.11, 25.93, 25.81, 25.66; ^{19}F NMR (376 MHz, CDCl3), δ (ppm): -62.62; ESI-MS $[M-Br]^+$ m/z calcd for $C_{37}H_{50}F_3N_4O_5^+Br^-$ 687.37278, found 687.37210.

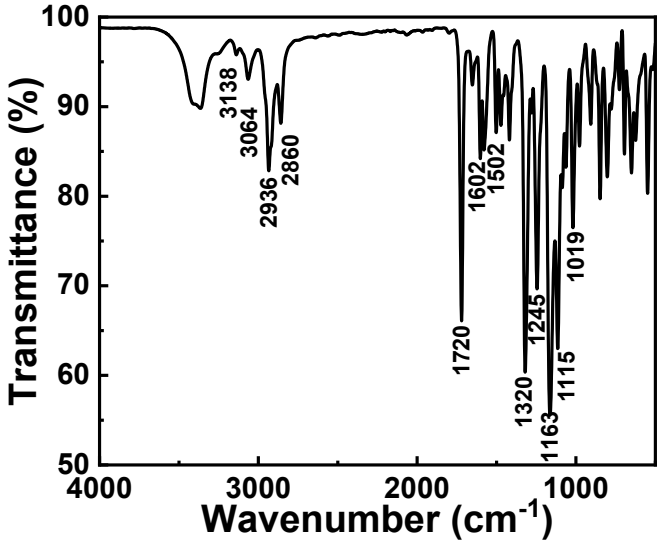

Fig. S2 FT-IR spectrum of the compound Azo1.

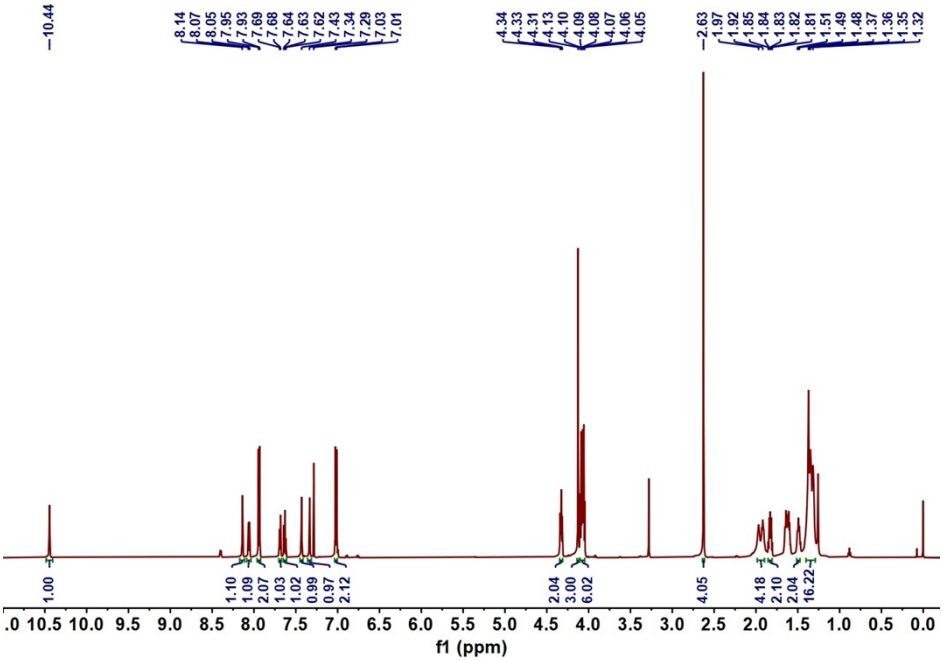

Fig. S3 [1] HNMR spectrum of the compound Azo1.

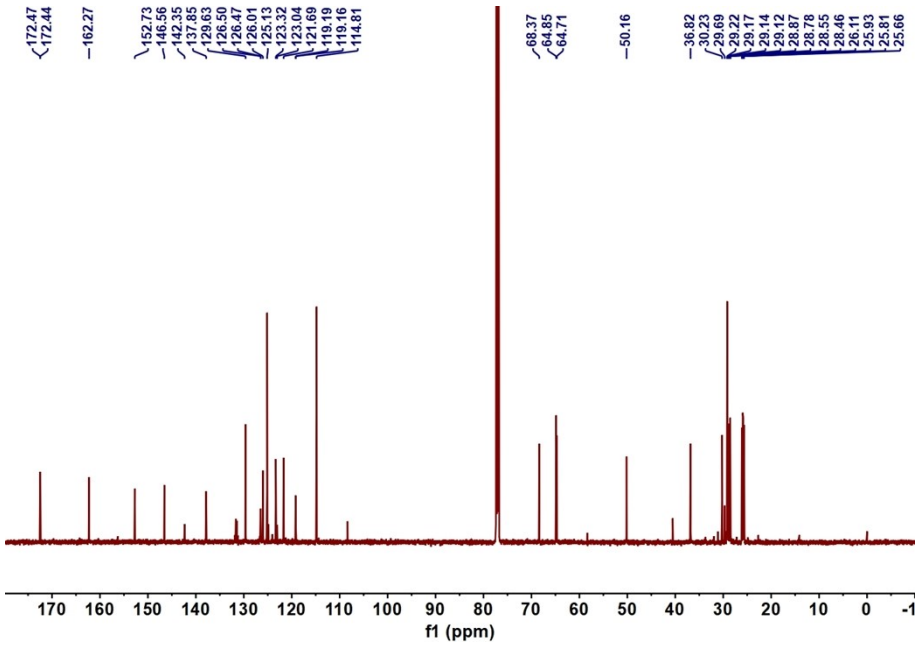

Fig. S4 [13] CNMR spectrum of the compound Azo1.

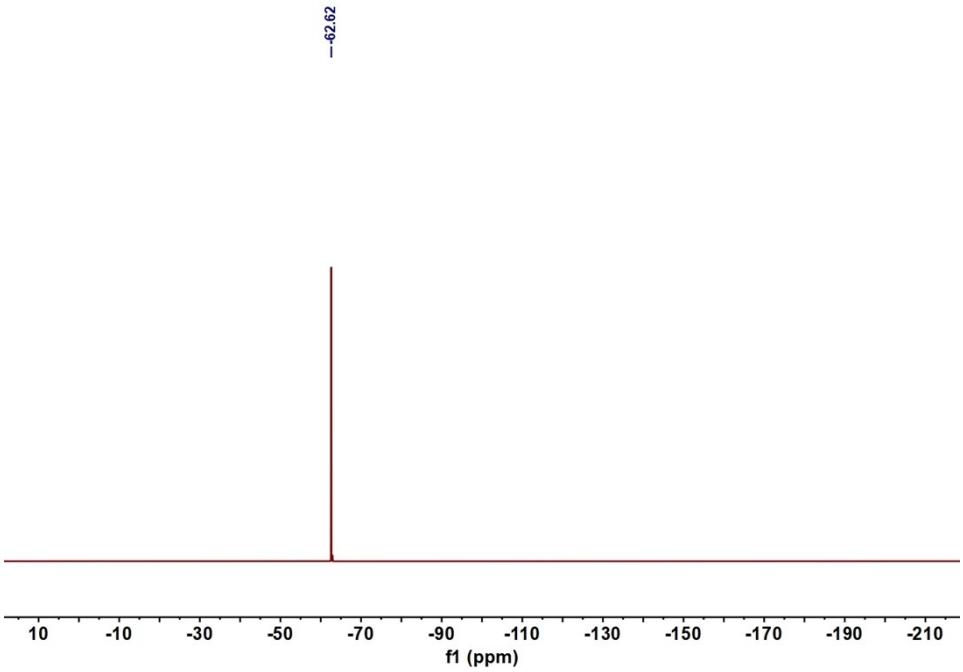

Fig. S5 [19] FNMR spectrum of the compound Azo1.

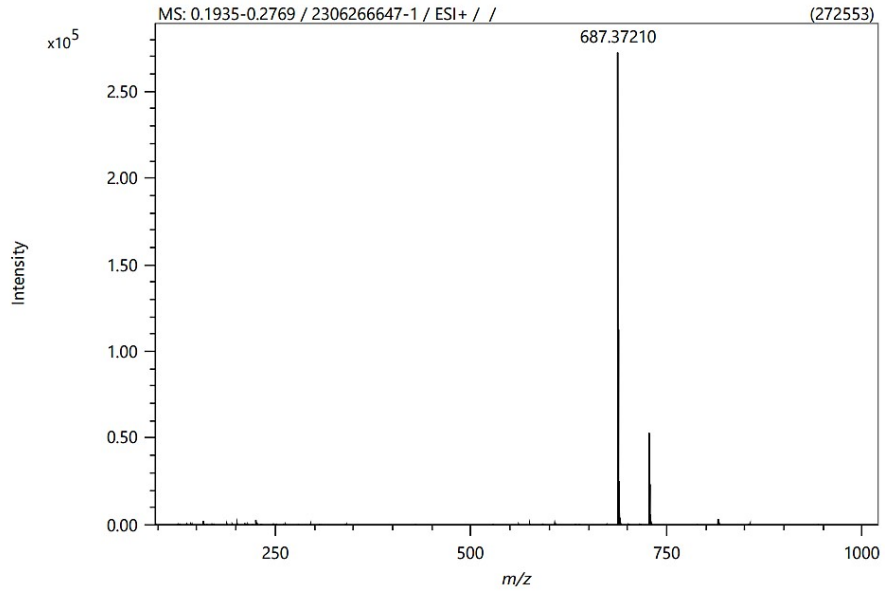

Fig. S6 MS spectrum of the compound Azo1.

Synthesis of AzoPc1

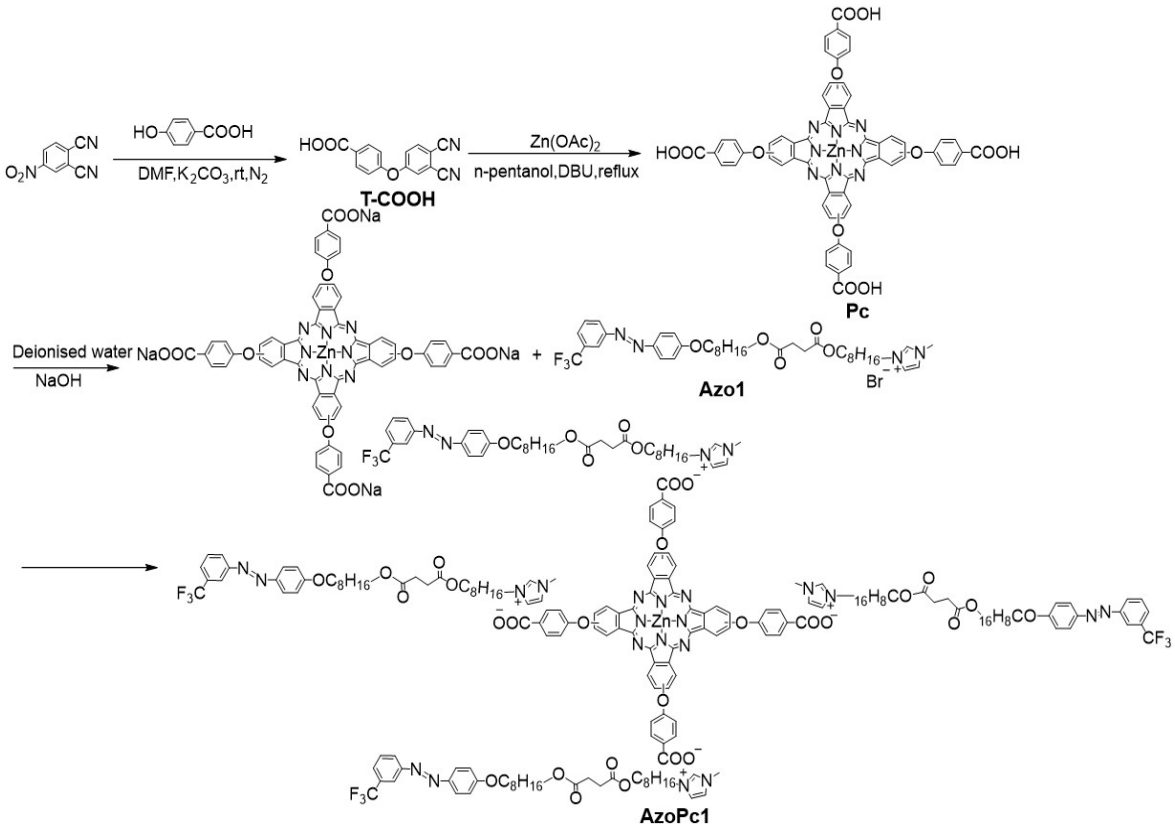

Fig. S7 Synthetic route of AzoPc1.

Synthesis of T-COOH

4-Nitrophthalonitrile (2.5 g, 14.45 mmol) was dissolved in 40 mL of DMF. Then, p-hydroxybenzoic acid (2 g, 14.45 mmol) and K_2CO_3 (4 g, 28.90 mmol) were added to the system, and the reaction was allowed to proceed for 16 h at the room temperature under the nitrogen protection. The reaction solution was poured into water to precipitate a solid powder and filtered. The filter cake was washed with ethanol several times, and the powder was dried to obtain T-COOH (2.70 g, yield 71.05%, m.p. 115-117 ^{o}C). FT-IR ν (cm^{-1}): 3086 (-OH), 2986 (-CH), 2230 (-C≡N), 1672 (-C=O), 1586 (benzene), 1424 (benzene), 1300 (-C-O), 1252 (benzene); ^{1}HNMR (400 MHz, DMSO-d6) δ ppm: 13.05 (s, 1H, -COOH), 8.16 (d, 1H, Ar-H), 8.04 (d, 2H, Ar-H), 7.94 (d, 1H, Ar-H), 7.54 (dd, 1H, Ar-H), 7.27 (d, 2H, Ar-H). ^{13}CNMR (151 MHz, DMSO-d6) δ ppm: 172.35, 162.59, 152.56, 137.60, 131.26, 130.77, 130.55, 127.34, 126.23, 125.51, 124.04, 123.45, 122.68, 118.06, 116.06.

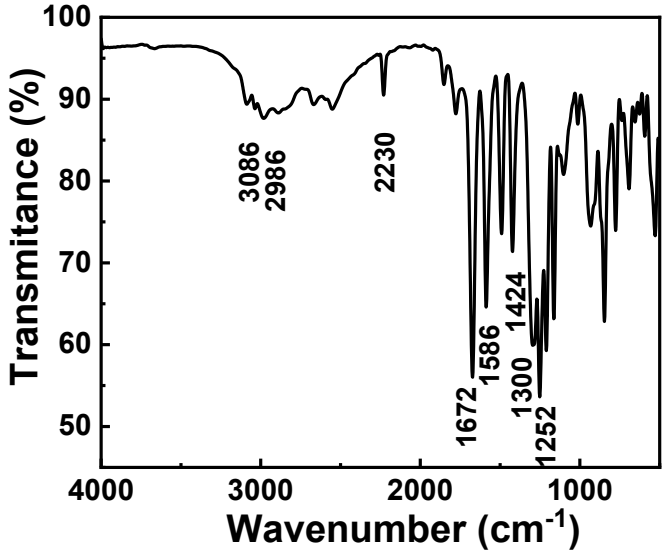

Fig. S8 FT-IR spectrum of the compound T-COOH.

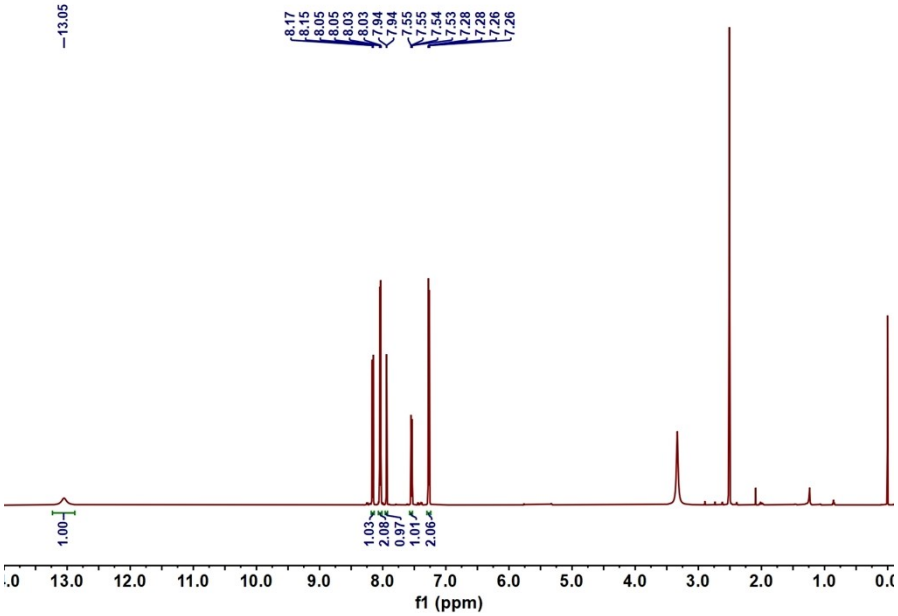

Fig. S9 [1] HNMR spectrum of the compound T-COOH.

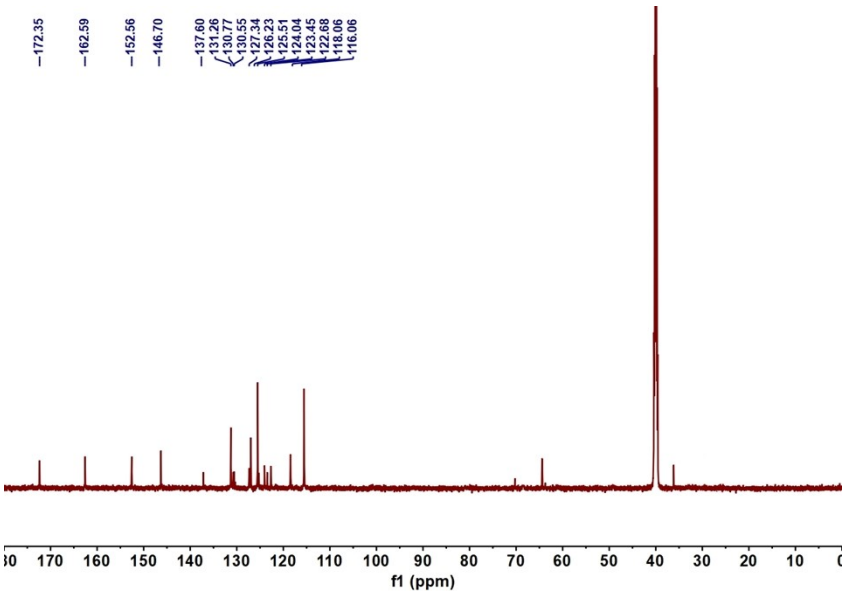

Fig. S10 ^{13}CNMR spectrum of the compound T-COOH.

Synthesis of Pc

T-COOH (2.0 g, 7.58 mmol) was dissolved in 20 mL of n-pentanol to which zinc acetate (1.39 g, 7.58 mmol) was added. The temperature was raised to 100 °C under the nitrogen protection and DBU (1.18 g, 7.58 mmol) was added, and the temperature was continued to 137 °C. The reaction was carried out for 24 h. After that, the mixture was poured into 50 mL of ethanol and filtered. The crude was washed with ethanol, ethyl acetate and dichloromethane for several times, and the powder was dried to obtain green powder Pc (1.64 g, yield 82.00%, m.p. >300 °C). FT-IR ν (cm^{-1}): 3259 (hydrogen bond), 2933 (-OH), 1715 (-C=O), 1598 (benzene), 1362 (benzene), 1299 (-C-O); ^{1}HNMR δ ppm (DMSO-d$_6$): 9.07 (s, 2H, Ar-H), 8.65 (s, 2H, Ar-H), 8.21-7.72 (m, 12H, Ar-H), 7.43 (dd, 8H, Ar-H), 7.23-7.11 (m, 4H, Ar-H). ^{13}CNMR (151 MHz, DMSO-d6) δ ppm: 169.35, 168.75, 167.34, 161.52, 139.70, 136.21, 132.30, 128.03, 125.68, 124.37, 121.23, 119.51, 118.99, 118.08, 113.68.

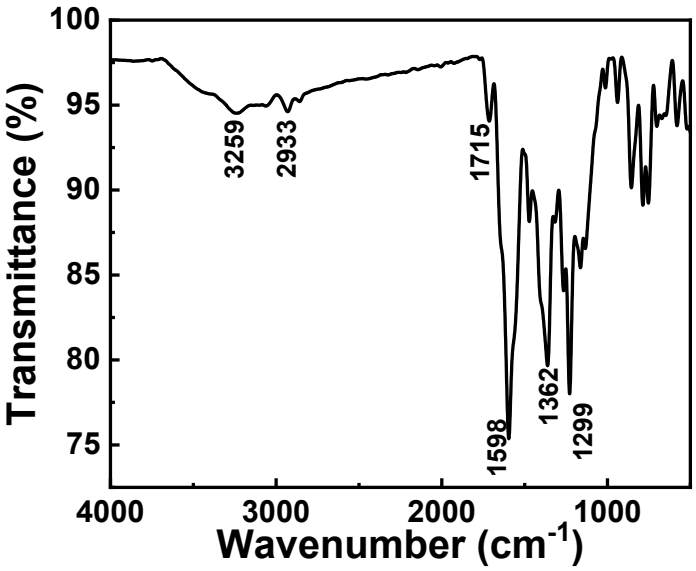

Fig. S11 FT-IR spectrum of the compound Pc.

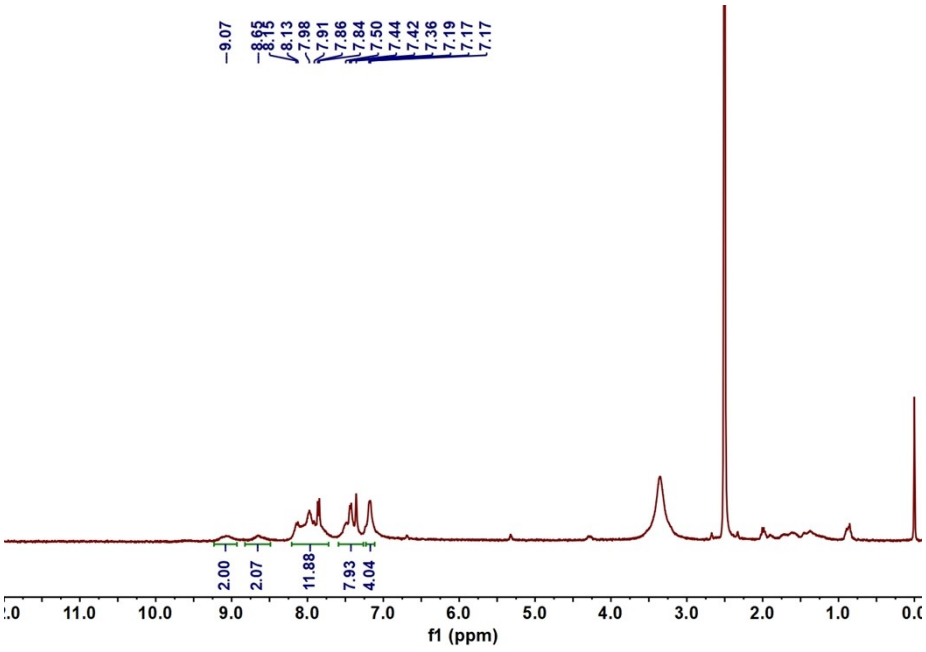

Fig. S12 [1] HNMR spectrum of the compound Pc.

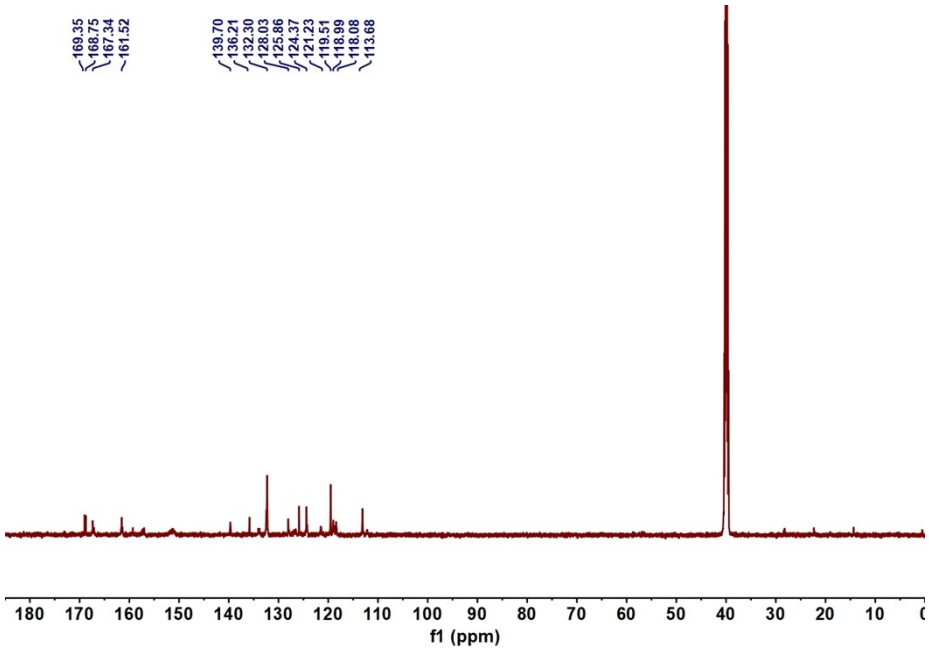

Fig. S13 ^{13}CNMR spectrum of the compound Pc.

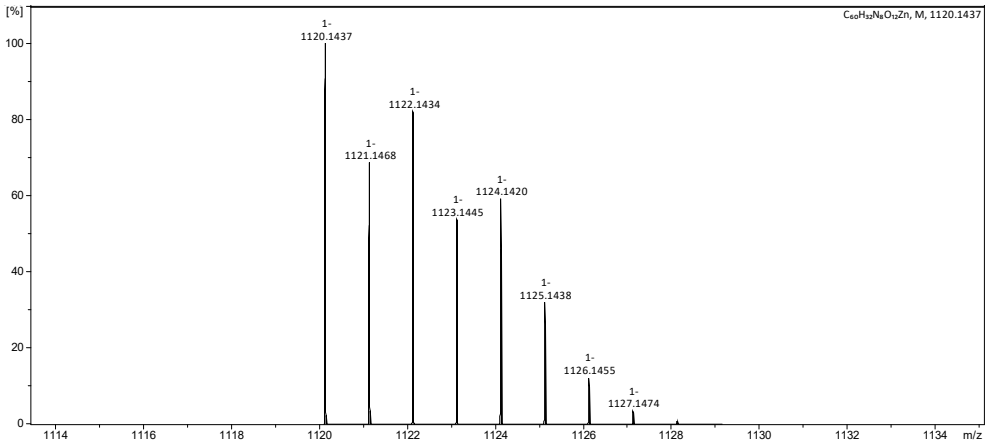

Fig. S14 MS spectrum of the compound Pc.

Synthesis of AzoPc1

Pc (0.11 g, 0.098 mmol) was added to 20 mL of the deionised water, and the pH value was adjusted to 12 with NaOH solution. Azo1 (0.30 g, 0.39 mmol) was dissolved in 20 mL of the deionised water and added to the alkaline solution of Pc. The green oily substance was precipitated by stirring for 2 h. The residue was poured into water and extracted with CH_2Cl_2. The organic phase was separated and washed with water three times. The combined organic phase was dried with anhydrous sodium sulfate. Hexane was added to the oil and sonicated to obtain a green powder. After standing, the supernatant was poured off and n-hexane was reintroduced, repeated 3-4 times and by the rotary evaporation to give AzoPc1 (0.36 g, yield 83.72%, m.p. 53-55 ^{o}C). FT-IR *v*

(cm^{-1}): 2932, 2858,1729, 1594, 1352, 1251, 1131,1062; ^{1}HNMR δ ppm (DMSO-d_6): 9.15 (s, 4H), 8.15 (d, 8H, Ar-H), 8.10 (s, 8H, Ar-H), 7.95 (d, 12H, Ar-H), 7.89 (d, 8H, Ar-H), 7.83 (s, 8H, Ar-H), 7.76 (s, 4H, Ar-H), 7.70 (s, 4H, Ar-H), 7.15 (d, 16H, Ar-H), 4.11 (dd, 16H,-CH_2-), 3.97 (dd, 16H, -CH_2-), 3.84 (s, 12H,-CH_3), 2.53 (s, 16H,-CH_2-), 1.75 (s, 16H,-CH_2-), 1.55 (d, 16H,-CH_2-), 1.42 (s, 24H,-CH_2-), 1.28 (d, 24H,-CH_2-). ^{13}CNMR (151 MHz, DMSO-d6) δ ppm: 172.35, 163.21, 151.97, 146.29, 137.16, 131.83, 130.77, 130.55, 127.34, 126.99, 125.51, 124.04, 123.45, 122.68, 118.48, 115.56, 70.25, 68.55, 65.12, 61.17, 49.16, 36.16, 34.70, 32.99, 30.28, 29.83, 29.37, 29.29, 29.09, 29.02, 28.97, 28.87, 28.70, 28.52, 28.50, 26.38, 26.36, 25.89, 25.80, 25.72, 25.66.

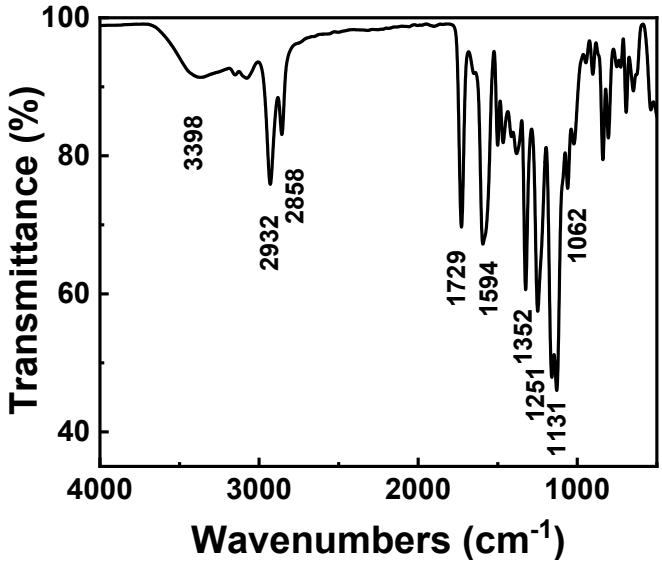

Fig. S15 FT-IR spectrum of the compound AzoPc1.

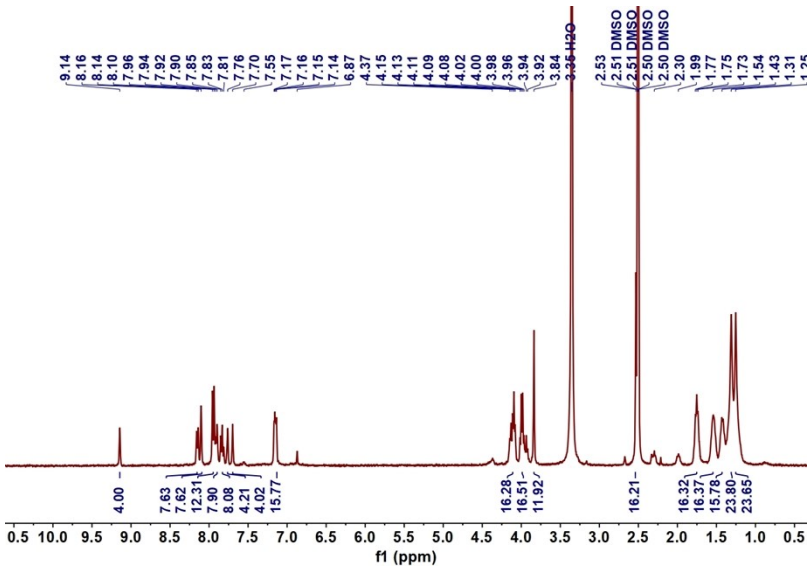

Fig. S16 [1] HNMR spectrum of the compound AzoPc1.

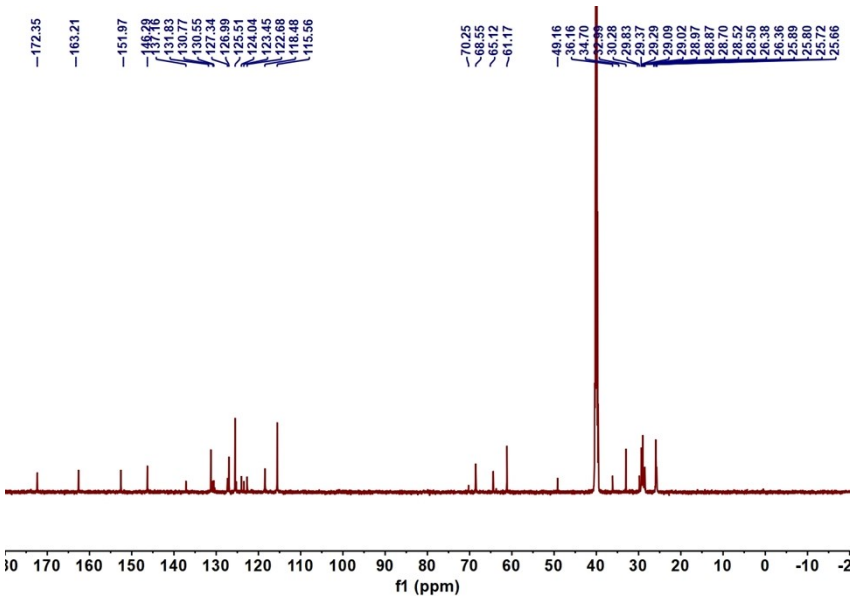

Fig. S17 [13] CNMR spectrum of the compound AzoPc1.

Fabrication of PVA@AzoPc1 and the Performances of the Smart Light-Driven Actuator. 5 g of polyvinyl alcohol (PVA) was added to 95 g of water and heated to dissolve, resulting in a 5% PVA solution. Subsequently, 0.0025 g of AzoPc1 was heated until melted and then added to 2 g of the PVA solution. The mixture was stirred for 12 h and allowed to defoam. Finally, the solution was poured into a mold and dried at 37 °C to produce a green transparent film, referred to as PVA@AzoPc1.

The PVA@AzoPc1 film (20 mm × 5 mm × 0.015 mm) was configured in an M-shape for the irradiation. The light source was placed on the right side of the M-shaped actuator and a camera was

used to record photos of the changes in the film at different light exposure times.

Fabrication of AzoPc1 Decorated Kapok Fibers (KF-PVA@AzoPc1) and Its Controllable Light-Driven Motion. The raw kapok fiber was initially degreased through the alkaline boiling. Kapok fibers (3 g) was added to 1% $NaClO_2$ (250 mL) and acetic acid (0.5 mL).The mixture was heated to 75 ^oC for 2 h and then washed several times with the ultrapure water until the solution reached neutral. Subsequently, the kapok fibers were soaked in 250 mL of 5% KOH for 24 h and then heated at 75 ^oC for an additional 2 h. The kapok fiber turned white, indicating that the lignin and wax had been completely removed. The solution was then washed with the ultrapure water, filtered and dried.

0.5 g of kapok fiber was mixed with 99.5 g of the ultrapure water and stirred for 24 h to create a 0.5 wt% KF dispersion. PVA solutions with different AzoPc1 content, 2.5%, 5.0%, 7.5% and 10.0%, were prepared relative to KF. Subsequently, 10 g of the KF dispersion were then added, followed by stirring for 6 h. The mixture was ultrasonicated to remove air bubbles, poured into a sand core funnel with a diameter of 4 cm and pumped. The resulting interfacial evaporation films based on KF were designated as KF-PVA@AzoPc1-1, KF-PVA@AzoPc1-2, KF-PVA@AzoPc1-3, and KF-PVA@AzoPc1-4, corresponding to the different contents of AzoPc1. Additionally, a control sample, consisting of KF that did not contain AzoPc1, was labeled KF-PVA. The actuators containing 10% Azo1 and Pc were prepared using the same method, labeled as KF-PVA@Azo1 and KF-PVA@Pc.

The KF-PVA @AzoPc1 film was cut into various shapes and placed on the surface of the water. A laser was directed at different positions of the actuator, while a camera recorded the trajectory of the actuator.

Photothermal Performance. The photothermal property was evaluated using an infrared imager to record the change of the surface temperature of the interfacial evaporated films. To investigate the effect of energy storage on the actuator's photothermal performance, the sample surface was initially irradiated with UV light (4.5 W m^{-2}) for 2 min to store energy. Subsequently, infrared light (1000 W m^{-2}) was employed to release the stored heat. The actuator was then allowed to cool to the room temperature, and the temperature changes during this process were recorded. For the sample without energy storage, it was irradiated with IR light for 3 min and then allowed to cool to the room temperature.

Light-Driven Water Evaporation. The water evaporation experiments were conducted using the photothermal effect. A beaker containing 10 mL of the deionized water was placed on a balance, and an interfacial evaporation actuator was floated in the water. Placed the IR light source on the top and recorded the water weight every minute. An UV light source was used to irradiate the interface of the evaporation films for 2 min, enabling the conversion of light energy into chemical energy, which was stored in the actuators. Subsequently, the recharged actuator was placed on the surface of a beaker containing the deionized water and continued to be irradiated with the IR light source. Similarly, the residual weight of the water was recorded every minute to evaluate the evaporation performance of the charged samples. To further simulate the evaporation performance under the natural conditions, a lamp (1000 W m^{-2}) was used to mimic the evaporation performance of sunlight on a continuously energized charge. The evaporation efficiency of water was assessed using the equation (1):

$$V = (m0 - mt)/St \quad (1)$$

where V is the evaporation efficiency of the films, m_0 is the initial total weight of the evaporated solution, m_t is the remaining weight of the evaporated solution, S is the treated area, and t is the heated time of the films.

Photodynamic and Photothermal Synergistic Self-Cleaning Antibacterial. Photodynamic antibacterial properties of the compounds in solution were determined according to the AATCC 100 standard. Staphylococcus aureus (ATCC-6538) or Escherichia coli (ATCC-8099) were used as representative Gram-positive and Gram-negative bacteria. A certain concentration of the cultured bacteria was diluted to 10^4 CFU mL^{-1} with phosphate buffered saline (PBS). Two pieces of the films (3 cm x 3 cm) were placed in sterile Petri dishes and filled with 0.15 mL of bacteria diluted to 10^4 CFU mL^{-1}, respectively. The samples were placed under the light or dark conditions for 10 min. The photodynamic antibacterial performance was investigated at 0 ^oC using 680 nm irradiation. Additionally, the synergistic antibacterial effects of photodynamic and photothermal processes were examined under 680 nm light irradiation. In this study, the interfacial evaporation film was initially energized with UV light before being irradiated with IR light to assess the combined photodynamic and photothermal antibacterial performance following the energization. The films were then immersed in 15 mL of PBS and the mixture was shaken for 2 min. 0.1mL of the mixture was removed and diluted 10, 10^2, 10^3 times and then inoculated onto agar medium and

incubated at 37 °C for 18 h or 10 h. The bacterial reduction rate was calculated in terms of the number of colonies according to the equation (2).

$$\text{Reduction of bacteria (\%)} = (R0 - R)/ R \times 100 \quad (2)$$

where R_0 and R are the number of colony-forming units of control (without agents) and the samples, respectively.

Characterizations. UV-visible absorption spectra were recorded on a Hitachi U-3310 Spectrophotometer (Hitachi Co., Ltd., Japan). Fourier transform infrared (FT-IR) spectra were measured using a PerkinElmer Spectrum Two equipped with an attenuated total reflectance (ATR) accessory (PerkinElmer Co., Ltd., USA). ^{1}HNMR spectra were recorded on Bruker Avance 400 (Bruker Co., Ltd., Switzerland) using DMSO-*d6* as a solvent. Optical microscope images were taken using a DM2700 P Leica Hot Stage Polarizing Microscope (Leica, Germany). Particle size was measured using a NANO ZS Nanoparticle Size Potential Meter (Malvern, UK). TEM images were obtained by JEM F200 Field Emission Transmission Electron Microscope (JEOL, Japan). The surface morphology of the films was obtained by a scanning electron microscopy (SEM, Hitachi, S-4800, Japan).

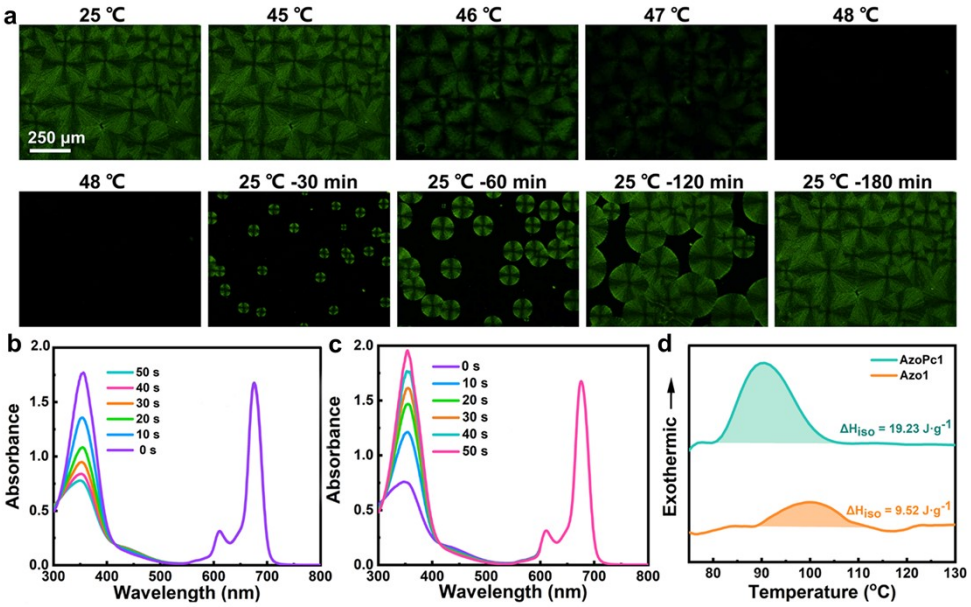

Fig. S18 The liquid crystal properties of the designed ionic liquid disk-like molecule. (a) The nematic liquid crystal texture (POM) during the heating and cooling process of AzoPc1. UV-vis absorption spectra of AzoPc1 under (b) UV (365 nm, 4.5 W m^{-2}) and (c) IR light irradiation (680 nm, 78.5 W m^{-2}). (d) DSC heating curves of AzoPc1 and Azo1 after charging under the UV light.

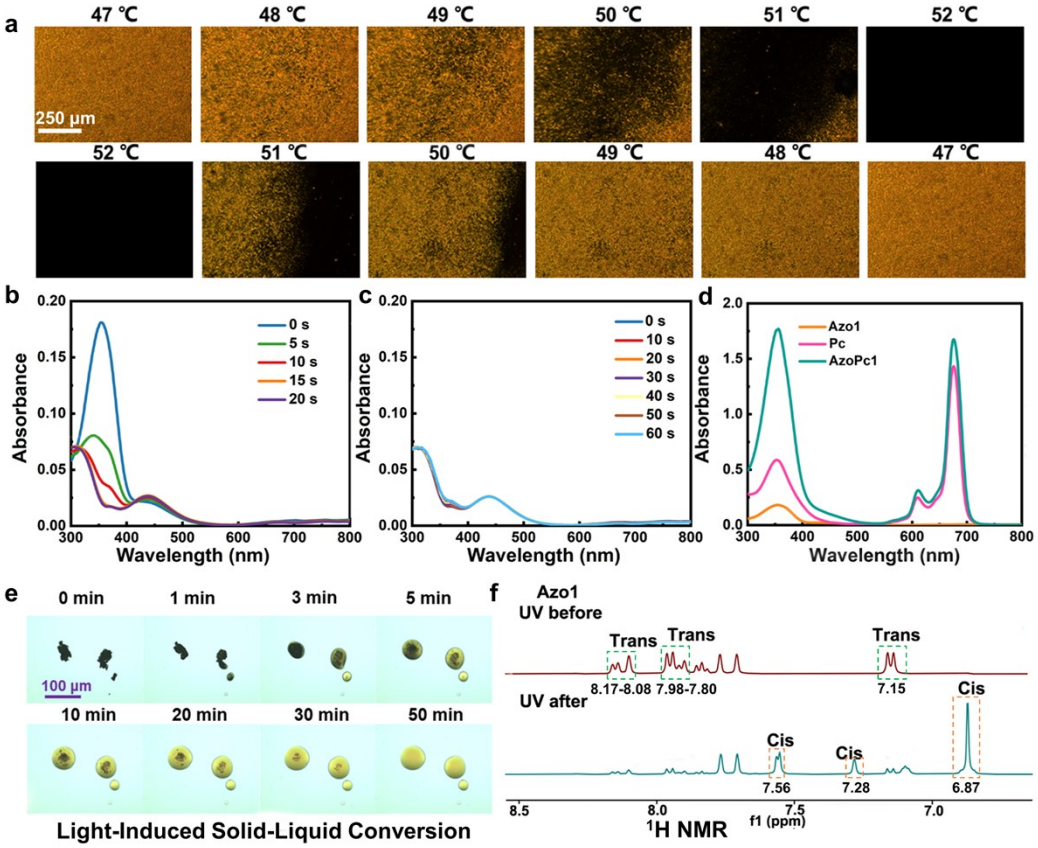

Fig. S19 Photoliquefaction and liquid crystal properties of Azo1. (a) Polarizing optical microscope (POM) images during the heating and cooling process of Azo1. (b) UV-vis absorption of Azo1, Pc and AzoPc1 (40 μmol·L^{-1}). UV-vis absorption spectra of Azo1 under (c) UV (365 nm, 4.5 W m^{-2}) and (d) IR light irradiation (680 nm, 78.5 W m^{-2}). (e) OM images of light-induced solid-liquid transitions of Azo1 under the different time UV irradiation. (f) ^{1}H NMR spectra of the initial Azo1 and after UV light.

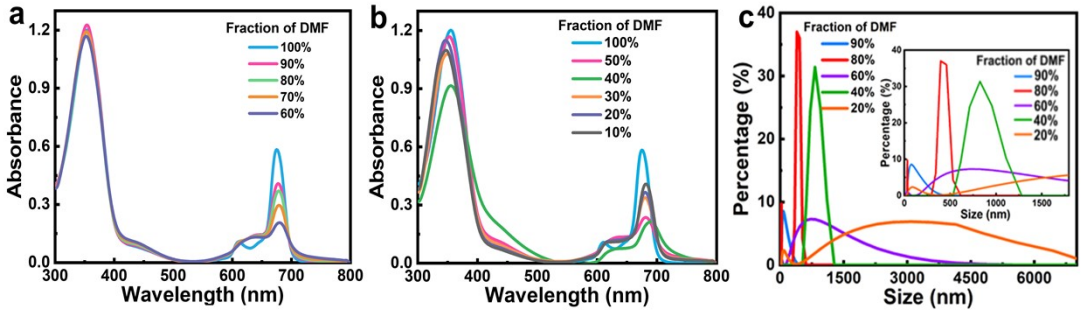

Fig. S20 Absorption spectra of AzoPc1 with different DMF and water contents: (a) and (b). (c) Size distribution of AzoPc1 with different DMF and water contents obtained by DLS.

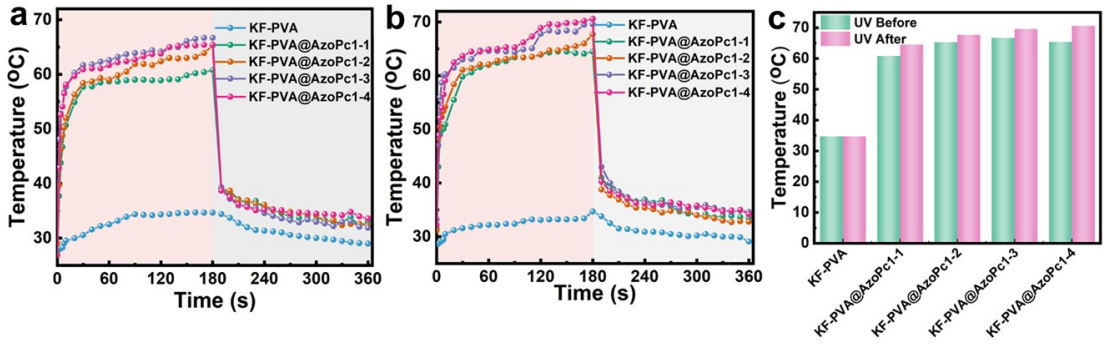

Fig. S21 Photothermal properties of KF-PVA@AzoPc1 before and after energy storage. The surface temperature curves of KF-PVA@AzoPc1 evaporators with the different content of AzoPc1 under (a) IR irradiation (1000 W m^{-2}) and (b) IR irradiation after 2 min of UV charging. (c) The change in maximum temperature of KF-PVA@AzoPc1 evaporators with the different content of AzoPc1 before and after charging, respectively.

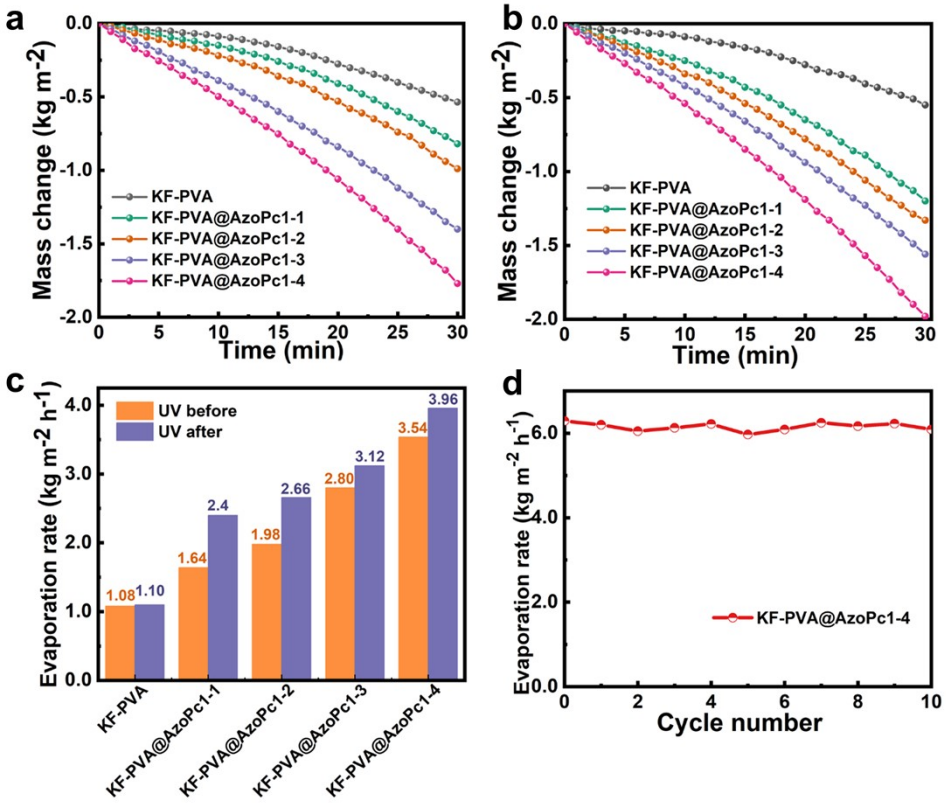

Fig. S22 Photothermal water evaporation properties of KF-PVA@AzoPc1 before and after the energy storage. Mass change curves of water for KF-PVA@AzoPc1 evaporators with the different content of AzoPc1 under (a) IR irradiation (1000 W m^{-2}) and (b) IR irradiation after 2 min of UV charging. (c) Evaporation rate of KF-

PVA@AzoPc1 evaporators with the different content of AzoPc1 under the various light conditions. (d) Evaporation rate during 10 cycles under the one-sun irradiation.

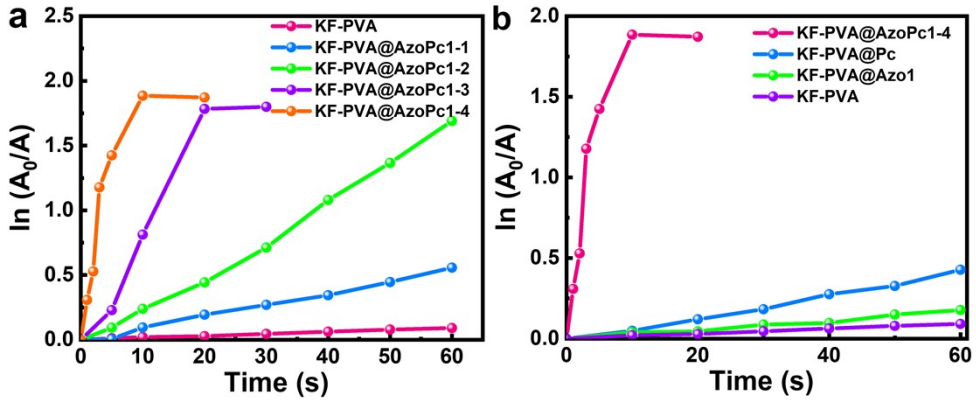

Fig. S23 Singlet oxygen generation performance of KF-PVA@AzoPc1. (a) Singlet oxygen production of KF-PVA@AzoPc1 with the different content of AzoPc1. (b) Singlet oxygen production of KF-PVA, KF-PVA@Azo1, KF-PVA@Pc and KF-PVA@AzoPc1-4, respectively.

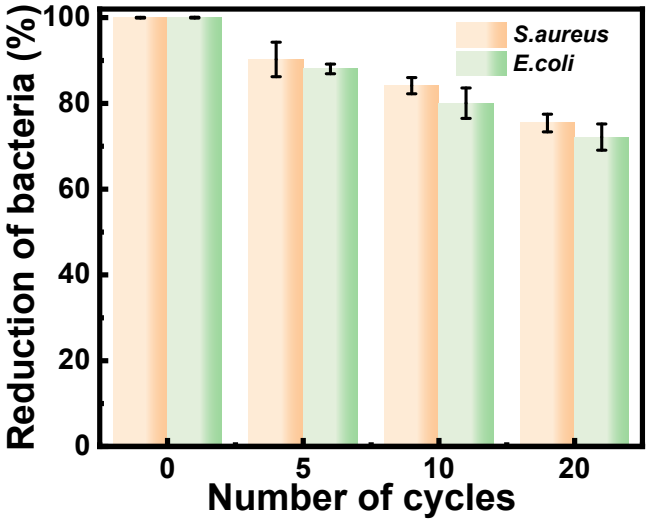

Fig. S24. The photodynamic antibacterial rates of KF-PVA@AzoPc1-4 after cycles for 5, 10, and 20 times.